

## Nuclear halo structure and pseudospin symmetry

Wen Hui Long (龙文辉),<sup>1,2,3,4,\*</sup> Peter Ring,<sup>2</sup> Jie Meng (孟杰),<sup>3</sup> Nguyen Van Giai,<sup>5,6</sup> and Carlos A. Bertulani<sup>4</sup>

<sup>1</sup>*School of Nuclear Science and Technology, Lanzhou University, 730000 Lanzhou, People's Republic of China*

<sup>2</sup>*Physik-Department der Technischen Universität München, D-85748 Garching, Germany*

<sup>3</sup>*School of Physics, Peking University, 100871 Beijing, People's Republic of China*

<sup>4</sup>*Department of Physics, Texas A&M University, Commerce, Texas 75429, USA*

<sup>5</sup>*CNRS-IN2P3, UMR 8608, F-91406 Orsay, France*

<sup>6</sup>*Université Paris-Sud, F-91405 Orsay, France*

(Received 24 November 2009; published 31 March 2010)

Nuclear halo structure and conservation of relativistic symmetry are studied within the framework of the relativistic Hartree-Fock-Bogoliubov theory. Giant halos as well as ordinary ones are found in cerium isotopes close to the neutron drip line. Bridged by the  $T = 0$  channel, the conservation of pseudospin symmetry (PSS) plays an essential role in stabilizing the neutron halo structures. The Fock terms, especially the  $\rho$ -tensor couplings, not only play a significant role in PSS conservation but also present substantial contributions to the  $T = 0$  channel, by which the necessity of Fock terms is well demonstrated.

DOI: [10.1103/PhysRevC.81.031302](https://doi.org/10.1103/PhysRevC.81.031302)

PACS number(s): 21.30.Fe, 21.60.Jz, 24.10.Cn, 24.10.Jv

Because the neutron halo was first proven to exist in  $^{11}\text{Li}$  [1], unexpected exotic modes have greatly challenged our understanding of exotic nuclei with an extreme neutron-to-proton ratio, which play an essential role in the evolution of the universe. In the typical exotic mode, the nuclear halo (see Refs. [2–5] and references therein)—the extremely diffuse matter—may strongly enhance the reaction cross section, which is of special significance for element synthesis in astrophysics as well as for the discovery of new superheavies. Accompanying nuclear halo occurrence, shell quenching [6,7] has been found when approaching these exotic regions, for example, the  $N = 8$  shell in Li.

The nucleon-nucleon ( $NN$ ) interaction is originally caused by meson exchange processes as predicted by Yukawa [8]. Within this approach nuclear binding is achieved mainly by the equilibrium between the scalar (phenomenological  $\sigma$ ) and the vector ( $\omega$ ) meson fields [9], whereas the tensor forces owing to  $\rho$  and  $\pi$  meson exchanges take part in the shell structure evolution [10]. As a relativistic symmetry in the Dirac equation [11], pseudospin symmetry (PSS) [12,13] is an important general feature in the nuclear energy spectra. Its origin owes to a Lorentz scalar potential ( $\sigma$  field) and a Lorentz vector potential (time component of the  $\omega$  field) equal in magnitude, but opposite in sign [14]. In fact, the competition of large scalar and vector fields in nuclei naturally explains the spin-orbit potential [15], which makes exploration in exotic regions more reliable.

In exotic nuclei the valence neutrons or protons are loosely bound and their coupling with the continuum becomes important. In terms of Bogoliubov quasiparticles, the relativistic Hartree-Bogoliubov (RHB) theory [15–17] provides a unified and self-consistent description of both mean field and pairing correlations and automatically takes continuum effects into account. Besides  $^{11}\text{Li}$  [18], the halo phenomena have been predicted by the RHB theory in Ne [19,20], Na [20,21], and

Ca [22] isotopes. Giant halo structures in Zr isotopes have also been studied within the RHB framework [23] as well as in the nonrelativistic Hartree-Fock-Bogoliubov method [24].

While limited by the Hartree approach, important ingredients such as the *spin-dependent* tensor forces are missing in the RHB theory. In the density-dependent relativistic Hartree-Fock (DDRHF) theory [25,26], the tensor forces owing to  $\pi$  and  $\rho$  meson exchanges can be naturally taken into account and this has made significant improvements in the consistent description of shell evolution [27] and appropriate conservation of PSS [26,28]. In this work, we use cerium isotopes to study the nuclear halo phenomenon and relevant conservation of PSS within the relativistic Hartree-Fock-Bogoliubov (RHFB) theory [29], an extension of the DDRHF. For cerium isotopes the proton number  $Z = 58$  is closely related to the pseudospin partner states  $\pi 1\tilde{f}$  ( $\pi 1g_{7/2}$  and  $\pi 2d_{5/2}$ ), which represent well-conserved pseudospin symmetry either from the experimental data [30] or from the theoretical calculations [31]. As we will see, the corresponding PSS conservation is essential for the neutron shell effects when approaching the neutron drip line.

In Fig. 1 we show nuclear matter distributions (left) and neutron canonical single-particle configurations (right) for cerium isotopes close to the drip line. The neutron drip line calculated here with PKA1 [26] is  $N = 140$ , whereas the calculations with PKO1 [25] and DD-ME2 [33] predict a shorter one,  $N = 126$ . As shown in Fig. 1(a), the neutron densities become more and more diffuse after the isotope  $^{186}\text{Ce}$  ( $N = 128$ ), direct and distinct evidence of halo occurrence. From Fig. 1(b) we can see that such extremely extensive matter distribution, for example, in  $^{198}\text{Ce}$ , is mainly caused by the low- $l$  states, namely, the halo orbits  $\nu 4s_{1/2}$ ,  $\nu 3d_{5/2}$ , and  $\nu 3d_{3/2}$ . Seen from the occupations of the halo orbits  $N_{\text{halo}}$  in Fig. 1(d), the halos in  $^{186}\text{Ce}$ ,  $^{188}\text{Ce}$ , and  $^{190}\text{Ce}$  are ordinary, while  $^{192}\text{Ce}$ ,  $^{194}\text{Ce}$ ,  $^{196}\text{Ce}$ , and  $^{198}\text{Ce}$  presumably have giant halos because more than two neutrons occupy the halo orbits. Similar conclusions can also be obtained from the neutron numbers lying beyond a sphere of radius  $r = 10$  fm [ $N_{r>10\text{fm}}$  in Fig. 1(d)], which is large enough (the neutron matter radius

\*longwh@lzu.edu.cn

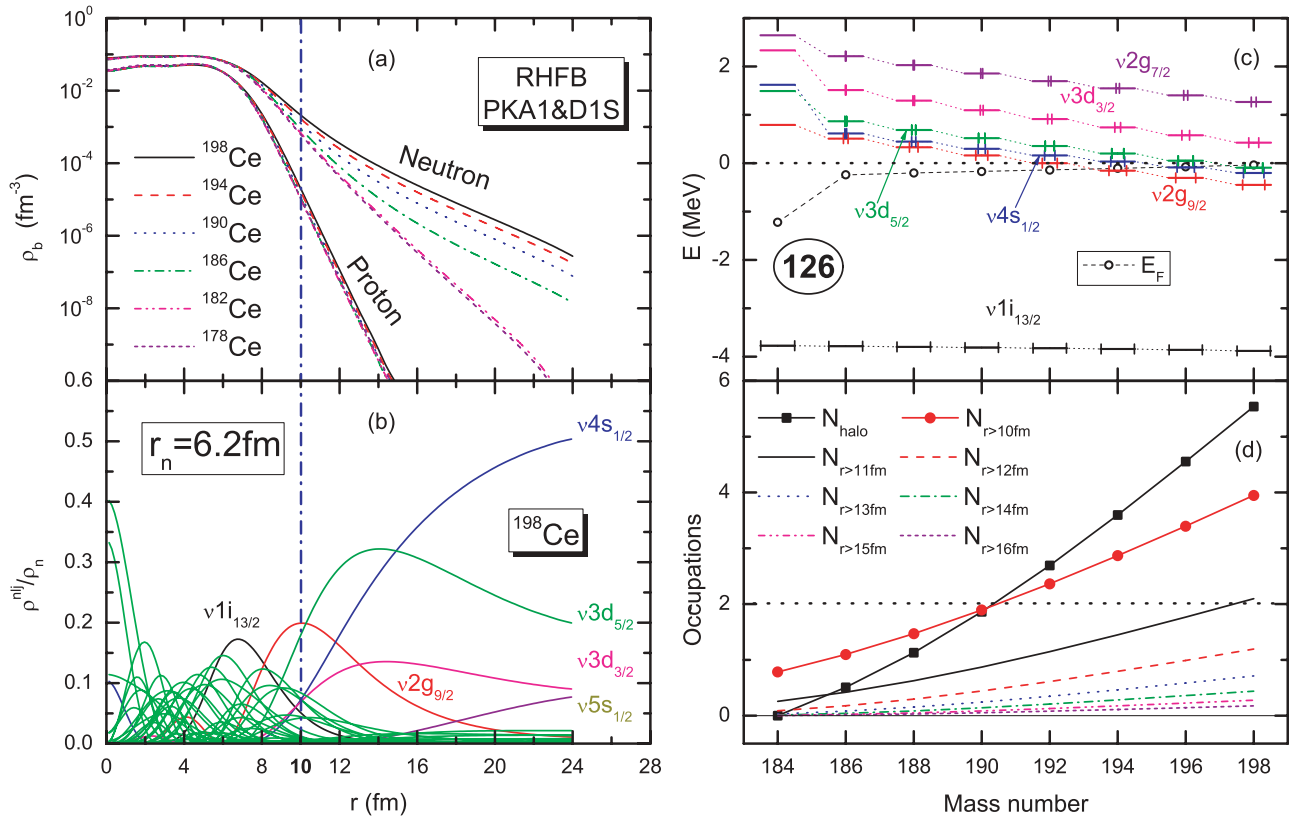


FIG. 1. (Color online) (a) Neutron and proton densities, (b) relative contributions of different orbits to the full neutron density in  $^{198}\text{Ce}$ , (c) neutron canonical single-particle energy, occupation probability ( $x$ -axis error bars), and Fermi energy  $E_F$  (open circles), and (d) neutron numbers filling the halo orbits  $4s_{1/2}$ ,  $3d_{5/2}$ , and  $3d_{3/2}$  ( $N_{\text{halo}}$ ) and those lying beyond the spheres with radii  $r = 10, 11, 12, 13, 14, 15$ , and  $16\text{fm}$ , respectively,  $N_{r>10\text{fm}}$ ,  $N_{r>11\text{fm}}$ ,  $N_{r>12\text{fm}}$ ,  $N_{r>13\text{fm}}$ ,  $N_{r>14\text{fm}}$ ,  $N_{r>15\text{fm}}$ , and  $N_{r>16\text{fm}}$ . Results were calculated by RHFb with PKA1 [26] plus the Gogny pairing force DIS [32]. The spherical box radius adopted was  $R_{\text{max}} = 28\text{fm}$ .

$r_n = 6.2\text{fm}$  in  $^{198}\text{Ce}$ ) for halos. Even extending to  $r = 16\text{fm}$ , which is sometimes taken as the radial cutoff in calculations of stable nuclei, a substantial number of neutrons still lies beyond this sphere in isotopes from  $^{192}\text{Ce}$  to  $^{198}\text{Ce}$ .

In Fig. 1(c) we find that the halo orbits ( $v4s_{1/2}$ ,  $v3d_{5/2}$ , and  $v3d_{3/2}$ ) are located around the particle continuum threshold where they are gradually occupied. For isotopes beyond  $^{184}\text{Ce}$  ( $N = 126$ ), the Fermi levels (open circles) approach the continuum threshold rather closely such that the stability of these halo isotopes becomes sensitive to pairing effects. Near the low- $l$  states, we find the high- $l$  states  $v2g_{9/2}$  and  $v2g_{7/2}$ . Because of the relatively large centrifugal barrier for  $g$  orbits, they do not contribute much to the diffuse neutron distributions. Nonetheless, the existence of high- $l$  states near halo orbits is particularly significant, because it leads to a rather high level density around the Fermi surface, and evidently the pairing effects are enhanced to stabilize the halo isotopes.

Evidence for the existence of a halo can also be found by studying the systematic behavior of nuclear bulk properties such as radii. In Fig. 2 we show the isospin dependence of the neutron skin thickness ( $r_n - r_p$ ) calculated in RHFb theory using the parameter set PKA1 for Ca, Ni, Zr, Sn, and Ce isotopes. With respect to the behavior in the stable region (dotted lines in Fig. 2), continuously growing deviations are found in the chains of Ca, Zr, and Ce until the neutron drip

line. This can be considered evidence of a halo. Despite the deviations in the midregion, Ni and Sn show an identical isospin dependence in both stable and neutron drip-line regions, which may indicate only a neutron skin, as the growth of a halo is interrupted. Compared with Ni, Sn isotopes show a much weaker skin effect.

Systematics similar to those in Fig. 2 are also found in RHB calculations for the chains of Ca and Zr [22,23]. For Ce isotopes the situation becomes quite different. RHFb calculations with the parameter set PKA1 (see Figs. 1 and 2) show clear evidence for the existence of halo structures in Ce isotopes, while in the calculations of RHFb with PKO1 [25] and RHB with DD-ME2 [33], the isotopic chain ends at  $N = 126$ , before the halo occurrence predicted by RHFb with PKA1. This deviation between models can be preliminarily interpreted by the shell structure evolution in Fig. 3(a), where much stronger shell effects are provided by PKO1 and DD-ME2 than by PKA1. As shown in Fig. 1(c), the neutron shell gap ( $N = 126$ ) between the  $v1i_{13/2}$  and the  $v2g_{9/2}$  states is close to the particle continuum threshold, which might essentially influence the stability of the drip-line isotopes.

In Fig. 3(b), the pseudospin orbital splitting  $\Delta E_{\pi 1\bar{j}}$  given by PKA1 shows an isospin dependence consistent with the neutron shell evolution, whereas in the results with PKO1

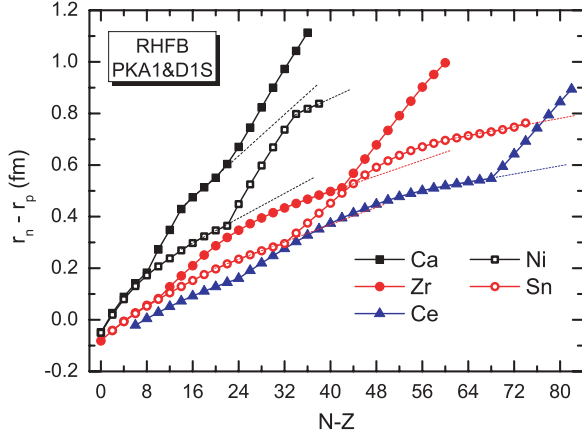


FIG. 2. (Color online) Neutron skin thickness  $r_n - r_p$  (fm) for Ca, Zr, Ni, Sn, and Ce as a function of isospin ( $N - Z$ ).  $r_n$  and  $r_p$  are the neutron and proton root mean square radii, respectively. Results were calculated by RHFb with PKA1 [26] plus the pairing force D1S [32].

and DD-ME2 such consistency is destroyed by the violation of PSS on the pseudospin partner states  $\pi 1\tilde{f}$ . To clarify this consistency between neutron shell evolution and proton PSS conservation we present in Fig. 4 the two-body interaction matrix elements  $V_{ab}$  calculated with PKA1 and responsible for the coupling between the proton [*a*:  $\pi 2d_{5/2}$  (filled symbols) and  $\pi 1g_{7/2}$  (open symbols)] and the neutron [*b*:  $v2f_{7/2}$ ,  $v2f_{5/2}$ ,

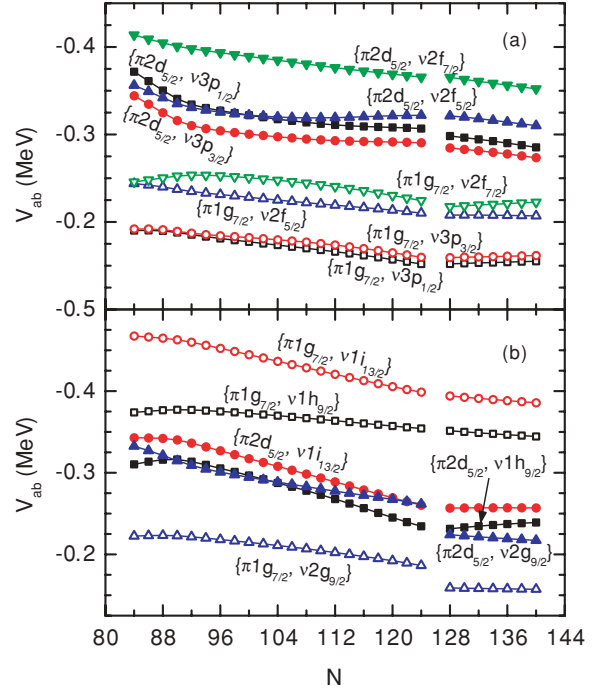


FIG. 4. (Color online) Two-body interaction matrix elements  $V_{ab}$ . Notation is as follows: *a* =  $\pi 2d_{5/2}$  (filled symbols) and  $\pi 1g_{7/2}$  (open symbols); *b* =  $v3p_{1/2}$ ,  $v3p_{3/2}$ ,  $v2f_{5/2}$ , and  $v2f_{7/2}$  (a); and *b* =  $v1h_{9/2}$ ,  $v1i_{13/2}$ , and  $v2g_{9/2}$  (b). Results correspond to RHFb with PKA1 plus the pairing force Gogny D1S.

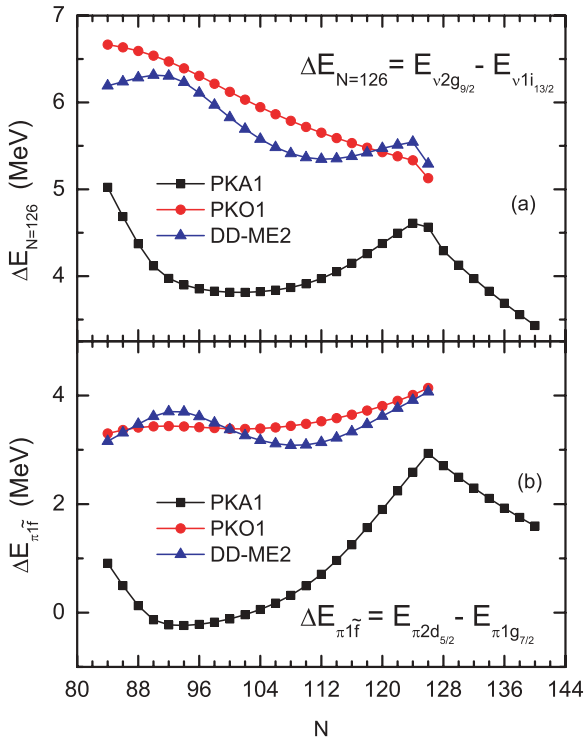


FIG. 3. (Color online) (a) Neutron shell gap at  $N = 126$  ( $\Delta E_{N=126} = E_{v2g_{9/2}} - E_{v1i_{13/2}}$ ) and (b) proton pseudospin orbital splitting ( $\Delta E_{\pi 1\tilde{f}} = E_{\pi 2d_{5/2}} - E_{\pi 1g_{7/2}}$ ) as functions of neutron number  $N$  for cerium isotopes. Results were calculated by RHFb with PKA1 [26], PKO1 [25], and RHFb with DD-ME2 [33]. The Gogny force D1S [32] was adopted in the pairing channel.

$v3p_{3/2}$ , and  $v3p_{1/2}$  in Fig. 4(a), and  $v1h_{9/2}$ ,  $v1i_{13/2}$ , and  $v2g_{9/2}$  in Fig. 4(b)] valence orbits. It is shown that the neutron orbits with nodes ( $v2f_{7/2}$ ,  $v2f_{5/2}$ ,  $v3p_{3/2}$ ,  $v3p_{1/2}$ , and  $v2g_{9/2}$ ) show stronger coupling with the proton  $\pi 2d_{5/2}$  than with the  $\pi 1g_{7/2}$  orbit, while those without nodes ( $v1h_{9/2}$  and  $v1i_{13/2}$ ) exhibit the opposite trend.

From  $^{142}\text{Ce}$  ( $N = 84$ ) to  $^{148}\text{Ce}$  ( $N = 90$ ) the valence neutrons mainly fill the  $v2f_{7/2}$  orbit, which leads to a corresponding recovery of PSS, as shown in Fig. 3(b). After  $^{148}\text{Ce}$  the orbit  $v1h_{9/2}$ , which has a stronger coupling with the  $\pi 1g_{7/2}$  than with the  $\pi 2d_{5/2}$  orbit, starts to be gradually occupied. The PSS on  $\pi 1\tilde{f}$  is still well preserved over a fairly long range from  $N = 90$  to  $N = 110$ , owing to the equilibrium between the states with nodes ( $v2f_{7/2}$ ,  $v2f_{5/2}$ ,  $v3p_{3/2}$ ,  $v3p_{1/2}$ ) and the one without a node ( $v1h_{9/2}$ ). From  $N = 112$  to  $N = 126$ , valence neutrons fill the  $v1i_{13/2}$  level, as the orbits below are nearly fully occupied. An increase in  $\Delta E_{\pi 1\tilde{f}}$  is therefore found [see Fig. 3(b)]. Upon approaching the neutron drip line, the state  $v2g_{9/2}$  starts to be occupied, and the levels below that are fully occupied. This leads to the continuous recovery of PSS after  $^{184}\text{Ce}$ . In fact, not only the  $v2g_{9/2}$  state, but also the other valence orbits beyond  $N = 126$  play a positive role in PSS recovery. From Figs. 3 and 4 one can see that the nodal structure shows substantial effects in determining the  $NN$  interaction strength and, further, plays an essential role in recovering PSS. In fact we also found similar nodal effects, as shown in Fig. 4, from the calculations with PKO1 and DD-ME2, while the unphysically large gap between  $\pi 1g_{7/2}$  and  $\pi 2d_{5/2}$  breaks the consistency (see Fig. 3)

TABLE I. Two-body interaction matrix elements  $V_{ab}$  (MeV) between proton and neutron valence orbits in  $^{198}\text{Ce}$ , as well as ratios of contributions from different coupling channels. The last four columns list the detailed Fock contributions, respectively, from  $\rho$ -vector ( $\rho$ -V),  $\rho$ -vector-tensor ( $\rho$ -VT),  $\rho$ -tensor ( $\rho$ -T), and  $\pi$ -pseudovector ( $\pi$ -PV) couplings. Results correspond to RHFB with PKA1 plus the pairing force Gogny D1S.

$b$	$V_{ab}$	$V_{ab}^D$	$V_{ab}^E$	$\rho$ -V	$\rho$ -VT	$\rho$ -T	$\pi$ -PV
$a = \pi 2d_{5/2}$							
$\nu 1i_{13/2}$	-0.257	63.2%	36.8%	9.7%	-4.0%	29.1%	2.1%
$\nu 2g_{9/2}$	-0.217	64.6%	35.4%	8.9%	-3.5%	27.0%	3.0%
$\nu 4s_{1/2}$	-0.097	71.8%	28.2%	7.1%	-4.4%	21.5%	3.9%
$\nu 3d_{5/2}$	-0.158	68.4%	31.6%	8.9%	-5.4%	25.7%	2.5%
$\nu 3d_{3/2}$	-0.156	67.7%	32.3%	7.9%	-5.4%	22.4%	7.4%
$\nu 2g_{7/2}$	-0.159	56.8%	43.2%	9.3%	-8.1%	30.8%	11.3%
$a = \pi 1g_{7/2}$							
$\nu 1i_{13/2}$	-0.386	63.5%	36.5%	8.3%	-4.4%	22.9%	9.8%
$\nu 2g_{9/2}$	-0.157	64.1%	35.9%	8.1%	-6.3%	25.3%	8.8%
$\nu 4s_{1/2}$	-0.052	68.1%	31.9%	8.2%	-5.0%	25.2%	3.5%
$\nu 3d_{5/2}$	-0.078	67.8%	32.2%	7.9%	-5.7%	24.5%	5.6%
$\nu 3d_{3/2}$	-0.074	70.2%	29.8%	8.4%	-5.4%	25.9%	0.9%
$\nu 2g_{7/2}$	-0.138	69.0%	31.0%	9.2%	-5.0%	28.0%	-1.2%

because the valence protons can only occupy the  $\pi 1g_{7/2}$  orbit.

Comparing PKA1 to PKO1 and DD-ME2, one finds that the deviations on the neutron shell effects at  $N = 126$  in Fig. 3(a) are mainly caused by a proton influence, that is, PSS conservation. In Fig. 4(b) it is shown that protons occupying the  $\pi 1g_{7/2}$  level tend to enhance the neutron shell effects ( $\Delta E_{N=126}$ ), whereas much weaker effects are contributed by particles in the  $\pi 2d_{5/2}$  orbit. Because of the serious violation of PSS on  $\pi 1\tilde{f}$  given by PKO1 and DD-ME2, the valence protons occupy only the  $\pi 1g_{7/2}$  state and this greatly increases neutron shell effects. It results in interruption of the isotopic chain at  $N = 126$ . In contrast, the PSS is properly conserved by PKA1 such that the pseudospin partner states are simultaneously occupied and the occupations are changed consistently. This

explains well the consistency between neutron shell effects and proton PSS conservation in Fig. 3. Although some minor differences may exist on the neutron side between models, this would not cause any substantial changes.

Because PSS conservation is tightly related to neutron shell effects at  $N = 126$ , it is also essential for the stability of cerium halo structures. Such consistency is bridged by the coupling between valence neutrons and protons, that is, the  $NN$  interaction in the  $T = 0$  channel. In Table I it is reported that Fock terms present significant contributions to the  $T = 0$   $NN$  interaction, about 30% of the total in most cases. In the  $T = 0$  channel, Fock terms are completely managed by isovector mesons, mainly (about two-thirds) by the tensor  $\rho$ , which cannot be efficiently taken into account by the Hartree approach. From Table I one can see that the tensor  $\rho$  plays a significant role not only in conserving PSS [26] but also in bridging neutron halo structure and proton PSS recovery.

In summary, within the RHFB theory with density-dependent meson-nucleon couplings, we have studied nuclear halo phenomena occurring in cerium isotopes, the relevant PSS conservation, and the role of Fock terms therein. Giant halos as well as ordinary ones are found in the drip-line Ce isotopes. We also found that the stability of neutron halo structures is tightly related to PSS conservation on the proton side. The Fock terms, mainly the  $\rho$ -tensor couplings, make substantial contributions to the  $NN$  interaction in the  $T = 0$  channel, which accounts for the consistency between neutron halo structures and proton PSS conservation. In addition, the necessity of Fock terms, especially the tensor  $\rho$ , is well demonstrated, as such effects cannot be obtained efficiently with the Hartree approach.

W.H.L. would like to thank Professor H. Sagawa for fruitful discussions. This work was supported by the Alexander von Humboldt Foundation, Major State 973 Program 2007CB815000, the National Natural Science Foundation of China under Grant Nos. 10435010, 10775004, and 10221003, the US DOE under Grant Nos. DE-FG $\phi$ 2- $\phi$ 8ER41533 and DE-FC $\phi$ 2-07ER41588 (UNEDF, SciDAC-2), and the Research Corporation.

- [1] I. Tanihata, H. Hamagaki, O. Hashimoto, Y. Shida, N. Yoshikawa, K. Sugimoto, O. Yamakawa, T. Kobayashi, and N. Takahashi, Phys. Rev. Lett. **55**, 2676 (1985).
- [2] J. E. Howard, H. R. Dullin, and M. Horanyi, Phys. Rev. Lett. **84**, 3244 (2000).
- [3] P. Mueller, I. A. Sulai, A. C. C. Villari, J. A. Alcantara-Nunez, R. Alves-Conde, K. Bailey, G. F. Drake, M. Dubois, C. Eleon, G. Gaubert, R. J. Holt, R. F. Janssens, N. Lecesne, Z.-T. Lu, T. P. O'Connor, M.-G. Saint-Laurent, J.-C. Thomas, and L.-B. Wang, Phys. Rev. Lett. **99**, 252501 (2007).
- [4] V. Rotival and T. Duguet, Phys. Rev. C **79**, 054308 (2009).
- [5] V. Rotival, K. Bennaceur, and T. Duguet, Phys. Rev. C **79**, 054309 (2009).
- [6] J. Dobaczewski, I. Hamamoto, W. Nazarewicz, and J. A. Sheikh, Phys. Rev. Lett. **72**, 981 (1994).
- [7] B. Chen, J. Dobaczewski, K. L. Kratz, K. Langanke, B. Pfeiffer, F. K. Thielemann, and P. Vogel, Phys. Lett. B **355**, 37 (1995).
- [8] H. Yukawa, Proc. Phys. Math. Soc. Japan **17**, 48 (1935).
- [9] B. D. Serot and J. D. Walecka, Adv. Nucl. Phys. **16**, 1 (1986).
- [10] T. Otsuka, T. Suzuki, R. Fujimoto, H. Grawe, and Y. Akaishi, Phys. Rev. Lett. **95**, 232502 (2005).
- [11] J. N. Ginocchio, Phys. Rep. **414**, 165 (2005).
- [12] A. Arima, M. Harvey, and K. Shimizu, Phys. Lett. B **30**, 517 (1969).
- [13] K. Hecht and A. Adler, Nucl. Phys. A **137**, 129 (1969).
- [14] J. N. Ginocchio, Phys. Rev. Lett. **78**, 436 (1997).
- [15] J. Meng, H. Toki, S. G. Zhou, S. Q. Zhang, W. H. Long, and L. S. Geng, Prog. Part. Nucl. Phys. **57**, 470 (2006).
- [16] J. Meng, Nucl. Phys. A **635**, 3 (1998).
- [17] D. Vretenar, A. V. Afanasjev, G. A. Lalazissis, and P. Ring, Phys. Rep. **409**, 101 (2005).

- [18] J. Meng and P. Ring, Phys. Rev. Lett. **77**, 3963 (1996).
- [19] W. Pöschl, D. Vretenar, G. A. Lalazissis, and P. Ring, Phys. Rev. Lett. **79**, 3841 (1997).
- [20] G. A. Lalazissis, D. Vretenar, W. Pöschl, and P. Ring, Nucl. Phys. A **632**, 363 (1998).
- [21] J. Meng, I. Tanihata, and S. Yamaji, Phys. Lett. B **419**, 1 (1998).
- [22] J. Meng, H. Toki, J. Y. Zeng, S. Q. Zhang, and S. G. Zhou, Phys. Rev. C **65**, 041302(R) (2002).
- [23] J. Meng and P. Ring, Phys. Rev. Lett. **80**, 460 (1998).
- [24] M. Grasso, S. Yoshida, N. Sandulescu, and N. Van Giai, Phys. Rev. C **74**, 064317 (2006).
- [25] W. H. Long, N. V. Giai, and J. Meng, Phys. Lett. B **640**, 150 (2006).
- [26] W. H. Long, H. Sagawa, N. V. Giai, and J. Meng, Phys. Rev. C **76**, 034314 (2007).
- [27] W. H. Long, H. Sagawa, J. Meng, and N. V. Giai, Europhys. Lett. **82**, 12001 (2008).
- [28] W. H. Long, H. Sagawa, J. Meng, and N. V. Giai, Phys. Lett. B **639**, 242 (2006).
- [29] W. H. Long, P. Ring, N. V. Giai, and J. Meng, Phys. Rev. C **81**, 024308 (2010).
- [30] Y. Nagai, J. Styczen, M. Piiparinen, P. Kleinheinz, D. Bazzacco, P. V. Brentano, K. O. Zell, and J. Blomqvist, Phys. Rev. Lett. **47**, 1259 (1981).
- [31] W. H. Long, T. Nakatsukasa, H. Sagawa, J. Meng, H. Nakada, and Y. Zhang, Phys. Lett. B **680**, 428 (2009).
- [32] J. F. Berger, M. Girod, and D. Gogny, Nucl. Phys. A **428**, 23 (1984).
- [33] G. A. Lalazissis, T. Nikšić, D. Vretenar, and P. Ring, Phys. Rev. C **71**, 024312 (2005).